Fate and Transport of Hexavalent Chromium in Undisturbed Heterogeneous Soil

ARTICLE *in* ENVIRONMENTAL SCIENCE AND TECHNOLOGY · JULY 1999

Impact Factor: 5.33 · DOI: 10.1021/es981211v

6 AUTHORS, INCLUDING:

Phil Jardine
University of Tennessee
227 PUBLICATIONS **6,032** CITATIONS
SEE PROFILE

Scott Fendorf
Stanford University
268 PUBLICATIONS **10,578** CITATIONS
SEE PROFILE

Melanie Mayes
Oak Ridge National Laboratory
69 PUBLICATIONS **671** CITATIONS
SEE PROFILE

Scott C Brooks
Oak Ridge National Laboratory
135 PUBLICATIONS **1,950** CITATIONS
SEE PROFILE

Environ. Sci. Technol. **1999**, *33,* 2939−2944

Fate and Transport of Hexavalent Chromium in Undisturbed Heterogeneous Soil

P. M. JARDINE,*,† S. E. FENDORF,‡ M. A. MAYES,† I. L. LARSEN,† S. C. BROOKS,† AND W. B. BAILEY†

Environmental Sciences Division, Oak Ridge National Laboratory, P.O. Box 2008, Oak Ridge, Tennessee 37831-6038, and Department of Geological and Environmental Science, Stanford University, Palo Alto, California 94305-2115

The disposal of toxic metals [e.g., Cr(VI)] generated by the Department of Energy during the cold war era has historically involved shallow land burial in unconfined pits and trenches. The objectives of this study were to investigate the impact of coupled hydrologic and geochemical processes on the fate and transport of Cr(VI) in undisturbed soil cores obtained from a fractured, acidic inceptisol that are commonly used in the disposal of waste at the Oak Ridge National Laboratory. The mobility of Cr(VI) was significantly retarded relative to a nonreactive Br^- tracer, and the mobility decreased with increased loading of the solid phase with natural organic matter (NOM). A significant portion of added Cr(VI) did not elute from the columns, and X-ray absorption near-edge structure (XANES) revealed that both Cr(VI) and Cr(III) resided on the soil mineral surfaces. The reduction of Cr(VI) to Cr(III) was dramatically more significant on soils with higher levels of surface-bound NOM. This indicated that NOM was serving as a suitable reductant during Cr(VI) transport even in the presence of potentially competing geochemical oxidation reactions involving Cr. The redox reaction was catalyzed by the presence of soil mineral surfaces, and the reduced product Cr(III) was immobilized as a tightly bound moiety. The effectiveness of surface-bound NOM to reduce toxic Cr(VI) to Cr(III) under acidic conditions has important implications regarding the design and implementation of in situ remedial strategies.

Introduction

The reduction of Cr(VI) by a variety of inorganic and organic reductants has been recognized as an important remedial strategy targeted at contaminant immobilization (*1*−*7*). Fe(II)-bearing minerals are known to effectively reduce Cr(VI) to Cr(III) over time scales of hours to hundreds of hours (*8*−*11*). Soils and sediments within the vadose zone oftentimes do not contain sufficient amounts of naturally occurring inorganic reductants (e.g., Fe(II), H_2S/HS^-) to impact the redox state of Cr(VI). Aerobic soils and sediments more commonly contain appreciable natural organic matter (particulate, adsorbed, dissolved) which can potentially promote the reduction of Cr(VI) to the less soluble, less mobile Cr(III) species. More than 2 decades ago, Bartlett and Kimble (*12*) recognized that the potent carcinogen Cr(VI) was rapidly reduced to Cr(III) by soil organic matter under acidic conditions. These findings were consistent with the observations that Cr(VI) is reduced in bulk solutions by many classes of organic compounds such as alkanes, alcohols, aliphatic and aromatic acids, etc. (*13, 14*). However, Deng and Stone (*6, 7*) have shown that unlike Cr(VI) reduction in bulk solution, mineral surfaces common to soils and sediments catalyze the reduction of Cr(VI) by organic compounds. These findings have important implications on the success of in situ remedial strategies concerned with the immobilization of Cr.

Although several studies have investigated Cr(VI) mobility in shallow aquifers (*15, 16*) and repacked soil columns (*17*), our knowledge base regarding Cr(VI) fate and transport in undisturbed soils and sediments is virtually nonexistent. Research in this area is critical since Cr dynamics are influenced by coupled hydrologic, geochemical, and microbial processes. It is not well-known whether Cr(VI) can be reduced and immobilized in soils and sediments affected by preferential flow and competing geochemical oxidation reactions [reoxidation of Cr(III) products by MnO_2; see Fendorf and Zasoski (*18*)]. Therefore, our objective was to provide an improved understanding and predictive capability of Cr(VI) fate and transport in undisturbed, heterogeneous soils. We couple microscopic and macroscopic experimental techniques to quantify the rates and mechanisms of Cr dynamics in systems complicated by multiple hydrologic and geochemical processes.

Materials and Methods

Site Description and Sample Preparation. Undisturbed soil columns (8.5-cm diameter × 14.5-cm length) were isolated from a proposed solid waste storage area (Melton Branch Watershed) on the Oak Ridge Reservation (ORR) in eastern Tennessee. Soils in this area are weakly developed acidic inceptisols that have been weathered from interbedded shale−limestone sequences. The limestone has been weathered to massive clay lenses devoid of carbonate, and the more resistant shale has weathered to an extensively fractured saprolite. Fractures are highly interconnected and conducive to preferential flow. The soil matrix is highly porous with typical saturated soil water contents ranging from 30 to 50%. Select chemical and mineralogical characteristics of the two soils are provided in Table 1, and detailed information regarding site hydrodynamics and geochemistry can be found in Arnseth and Turner (*19*), Jardine et al. (*20*−*22*), Wilson and Luxmoore (*23*), and Wilson et al. (*24*−*26*). An important observation to note in these mixed systems is that the pore water pH is controlled by the clay lense material which has a lower pH than the shale.

Two undisturbed, cylindrical soil columns were obtained in close proximity to each other within the C horizon, 1.5 m from the ground surface. Our rationale for acquiring columns from this depth is related to historical waste disposal practices on the ORR involving shallow pits and trenches in the vadose zone. A massive hydraulic press was used to push 14.5 cm long and 8.5 cm diameter beveled steel casing into the soil. The soil disturbance and compaction were negligible due to the near-instantaneous placement of the casing and high water content of the soil. Further, experimental displacement results compared favorably with those obtained from columns extracted by the more laborious hand-sculpting method (*21, 27*). Columns were carefully dug from the ground and transported to the laboratory, where fritted glass end plates were sealed in good contact with the soil column ends.

* Corresponding author phone: (423)574-8058; fax: (423)576-8646; e-mail: ipj@ornl.gov.
† Oak Ridge National Laboratory.
‡ Stanford University.

10.1021/es981211v CCC: $18.00
Published on Web 07/29/1999

TABLE 1. Select Chemical and Mineralogical Characteristics of the Two Soil Types Found within the Undisturbed Columns

soil type	pH[a]	DCB extractable Fe,[b] g kg^{-1}	OM g kg^{-1}	mineralogy[c]
weathered shale	4.6	25	0.89	$I_{30}IS_{29}V_{25}S_{10}K_3Q_3$
clay lense	3.8	29.4	2.15	$S_{37}K_{25}I_{15}IS_{10}V_{10}Q_5$

[a] 2:1 10 mM $CaCl_2$:soil ratio. [b] Dithonite−citrate−bicarbonate method of Mehra and Jackson (*36*). [c] Mineralogy of <2-μm clay fraction. Numerical subscripts refer to weight percentage of each mineral in sample as determined by differential scanning calorimetry and X-ray diffraction. I = illite, V = vermiculite, K = kaolinite, S = smectite, Q = quartz, IS = interstratified (random interstratified kaolinite:smectite).

Contact of the fritted glass plates with the soil was assured using a small quantity of sand-sized quartz to fill the voids of the rough column boundaries. Low dead-volume Tempe cells (Soil Moisture Equipment Corp., Santa Barbara, CA) were bolted together and held the fritted glass plates securely to the column ends. Glass frits were of the coarse variety (25−50-μm pore diameter) and were used to ensure the even displacement of influent onto the soil column surface.

Miscible Displacement Experiments. Prior to the displacement experiments, soil columns were slowly saturated with 10 mM $CaCl_2$ (pH = 3.7) from the bottom. Columns were inverted so that flow occurred from upper to lower horizonal positions, as is the case in situ. A manipulation was performed on one of the columns where the solid phase was amended with natural organic carbon (NOM). Freeze-dried NOM from a wetlands pond in Georgetown, SC (*28*), was dissolved in 10 mM $CaCl_2$ to make a 300 mg of C L^{-1} solution. The wetland pond from which the solution-phase NOM was obtained drains a hardwood forest, and the "brown water" contains high levels of NOM (~66 mg of C L^{-1}). The chemical details of the NOM can be found in McCarthy et al. (*28*) and Gu et al. (*29*, *30*). Dissolved NOM was added to the soil at a pore water flux of 0.09 cm h^{-1}. The quantity of NOM added was based on NOM sorption isotherms for this soil (*31*) and was equivalent to that amount needed to saturate the sorption sites of the entire soil column solid phase. The total organic carbon analysis of the solid phase, after the Cr displacement experiment was terminated, demonstrated that the distribution of adsorbed NOM was not uniform (preferential loading in the first 10 cm). Nevertheless, the distribution was sufficient for our purposes, and we were able to enhance the amount of solid-phase carbon by an average of 2.2 times throughout the column. Following the NOM amendment, several pore volumes of 10 mM $CaCl_2$ were flushed through the column in preparation for the tracer injection.

Influent tracer solutions consisted of 0.5 mM Cr(VI) as K_2CrO_4, 3.75 mM Br^- as $CaBr_2$, μCi levels of radioactive ^{51}Cr(VI), and 8 mM $CaCl_2$ at pH 3.9 and an ionic strength of 0.03 M. Influent was introduced into the columns as pulse additions at a constant pore water flux of 0.0902 cm h^{-1}. The duration of the tracer pulse continued until a Cr(VI) breakthrough plateau was observed. At this point, the influent was changed to 10 mM $CaCl_2$, pH 3.9, and an ionic strength of 0.03 M. Pertinent physical characteristics of the column displacement experiments are provided in Table 2. Effluent was collected in automatic fraction collectors and analyzed for Br^- using ion chromatography (IC) and an ion-specific electrode, Cr(VI) using a modified *sec*-diphenylcarbazide procedure (*12*), total Cr by inductively coupled plasma (ICP) and atomic absorption spectrophotometry, ^{51}Cr using a high-purity intrinsic germanium (HPGe) coaxial detector, major cations and anions by ICP and IC, respectively, total dissolved organic carbon using high-temperature combustion, and pH by conventional methods. The untreated column (no added NOM) was leached until effluent Cr was <5% of the influent. The NOM amended column was terminated slightly before this point in order to ship the solid phase to the Stanford Synchrotron Radiation Laboratory (SSRL) for scheduled analysis.

Solid-Phase Analysis. Following the termination of each displacement experiment, the columns were dismantled and soil was extracted and sectioned from each core using a depth interval of approximately 1.5 cm. Solid-phase radioactive ^{51}Cr was quantified for each soil depth interval by direct counting using a HPGe coaxial detector. The sample containers were calibrated using a NIST traceable γ-ray standard solution (QCY series, Amersham, Inc.) in an aqueous matrix (*32*). This information coupled with effluent analyses resulted in a Cr mass balance of 99% and 88% for the untreated and NOM-amended soil columns, respectively. Solid-phase organic carbon was also quantified for each depth interval using a standard combustion technique. Solid-phase Cr was speciated using X-ray absorption near-edge structure (XANES) spectroscopy, which was conducted at the Stanford Synchrotron Radiation Laboratory (SSRL) under dedicated running conditions. Scans were recorded from −200 to 300 eV around the K-edge of chromium (5989 eV), with 0.2-eV steps across the white-line and main-edge region. Energy selection was accomplished with a Si(*220*) double-crystal monochromator, with a 1-mm (h) × 20-mm (w) beam. Absorption was measured by the proportional fluorescent X-ray production using a 13-element Ge detector (*33*). Mass fractions of Cr(III) and Cr(VI) were determined with depth for each column using XANES spectroscopy by sectioning the soil and placing it in a 4- × 4- × 40-mm slot cut in an acrylic plate that was sealed with Kapton. The proportion of Cr(VI) relative to total chromium was then determined by the ratio of the white-line amplitude to the total atomic cross section and comparison to standard curves as described by Patterson et al. (*34*). Soil water content and bulk density of each core were determined directly by measuring the soil volume and the saturated and dry soil mass of each column.

Modeling. Effluent Br^- and Cr(VI) were modeled using the multireaction transport model (MRTM) described by Selim et al. (*17*). The model is based on the one-dimensional convective−dispersive (CD) equation, and for our purposes, it was assumed that sorption sites could be distributed among two or three different forms. The two-site approach considered both equilibrium and irreversible first-order kinetic (k_{irr}) sites, and the three-site approach added a set of reversible first-order kinetic sites. Equilibrium sites had the option of considering either nonlinear sorption, expressed as the Freundlich equation (K and n as empirical parameters), or linear sorption where $n = 1$ and K becomes the equilibrium partitioning coefficient. Effluent Br^- was modeled with the nonreactive CD equation with optimization of the dispersion coefficient. Previous efforts have confirmed that Br^- does not adsorb onto these soils and remains nonreactive (O'Brien, 1994, ORNL, unpublished data). The dispersion coefficient determined for Br^- was assumed equivalent for Cr(VI) and was used in the reactive CD equation. Parameter unknowns included K, n, k_{irr}, and the adsorption and desorption rates on reversible first-order kinetic sites. Model-fitted values of k_{irr} provided an estimate of the quantity of Cr mass that was irreversibly sorbed to the solid phase, and this was compared to observed solid-phase ^{51}Cr. Model-fitted values of K and n were compared to values obtained from modeled batch equilibrium Cr(VI) adsorption isotherms determined on bulk soil from the site.

Results and Discussion

The breakthrough of Cr on the untreated soil core was delayed relative to nonreactive Br^-, suggesting significant retardation of the former by the solid phase (Figure 1A). Effluent Cr was

TABLE 2. Physical Parameters for the Column Displacement Experiments

column	tracers	water content, $cm^3\ cm^{-3}$	bulk density, $g\ cm^{-3}$	length, cm	radius, cm	pore water flux, $cm\ h^{-1}$	tracer pulse duration, h	Peclet no.[a]
untreated	Br, Cr(VI), ^{51}Cr(VI)	0.457	1.26	14.5	4.25	0.0902	2737	2.87 ± 0.48
NOM amended	Br, Cr(VI), ^{51}Cr(VI)	0.482	1.33	14.5	4.25	0.0902	4052	9.62 ± 3.37

[a] Peclet numbers were best fit to observed Br^- data using the convective−dispersive equation with the 95% confidence interval shown for the estimated value.

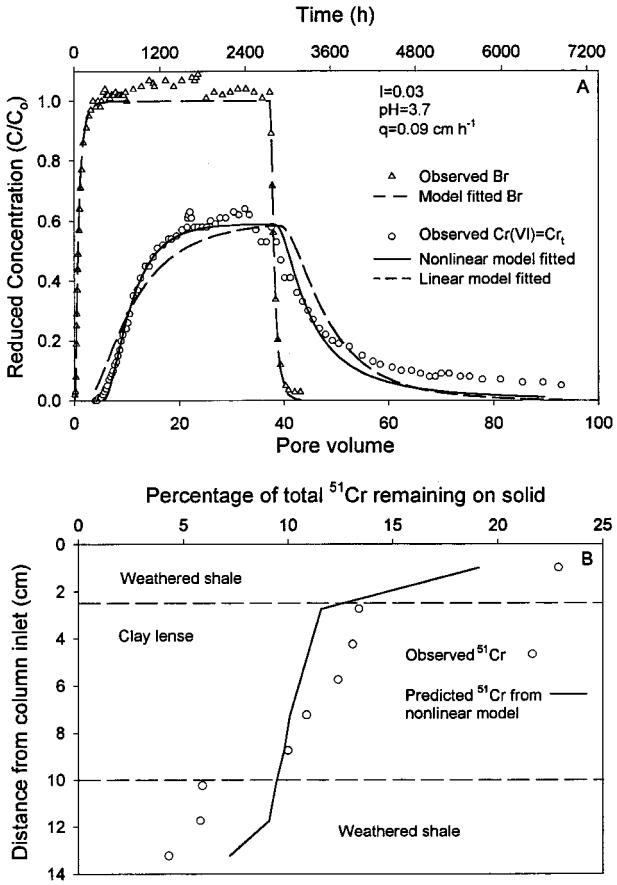

FIGURE 1. (A) Observed effluent Br^- and Cr(VI) with model-fitted curves using the multireaction transport model (MRTM) for an undisturbed soil column of interbedded weathered shale and clay lenses. Model input and output parameters are provided in Tables 2 and 3. (B) Observed and predicted distribution of ^{51}Cr (Cr(III) and Cr(VI)) within the undisturbed soil column.

entirely Cr(VI), and no Cr(III) was ever detected within experimental uncertainty. The radiotracer ^{51}Cr behaved identical to stable Cr(VI) since reduced effluent concentrations of $Cr_{total} = {}^{51}Cr = Cr(VI)$. The significance of Cr retardation by the solid phase is also evidenced by the fact that only 58.4% of the added Cr(VI) was eluted from the column. The remainder of the added Cr(VI) was associated with the solid phase, and this was substantiated by quantifying solid-phase ^{51}Cr (Figure 1B). The distribution of solid-phase Cr showed elevated levels near the column inlet that decreased sigmoidally with increasing distance into the core. The distribution of solid-phase Cr was surprisingly smooth and appeared influenced by the sharp boundaries imparted by the two significantly different interbedded soil types (Figure 1B).

Effluent Cr(VI) breakthrough curves (BTCs) were highly asymmetric, which is indicative of nonlinear sorption and/or kinetically limited sorption onto the solid phase (Figure 1A). Observed Cr(VI) effluent was modeled with MRTM (*17*) by initially assuming sorption sites could be distributed among two forms: equilibrium sites and irreversible first-order kinetic sites (k_{irr}). Both linear and nonlinear sorption was considered where the model best-fit K and k_{irr} for linear sorption and best-fit K, n, and k_{irr} for nonlinear sorption. Both situations provided reasonable fits to the observed Cr(VI) BTCs, with the nonlinear model fit providing an overall better description of Cr(VI) BTC asymmetry (Figure 1A, Table 3). These results are consistent with batch Cr(VI) sorption isotherms on these soils, which are nonlinear and well-described by the Freundlich equation (not shown). The magnitude of the batch K values, however, was significantly greater than for the undisturbed cores, which may have been the result of preferential bypass of a portion of the solid phase in the undisturbed columns (*20*). In contrast, model-fitted k_{irr} values provided an excellent estimate of the observed Cr mass that was irreversibly sorbed to the solid phase (Table 3). It is interesting to note that the k_{irr} values were similar in magnitude to those of Selim et al. (*17*) for Cr(VI) transport in packed beds of Cecil soil that had similar quantities of Fe−oxides and surface-bound NOM as our soils. The results may imply that the Cr(VI) immobilization rates determined in the current study may have application in subsoils from different regions that have comparable pH, organic matter, and Fe−oxide levels. The addition of another set of reversible first-order kinetic sites (three-site approach) did not significantly improve the model description of the observed data (not shown). Thus, the nonlinear nature of the adsorption process coupled with irreversible sorption kinetics adequately described Cr(VI) transport. Based on the nonlinear model fit to Cr(VI) effluent, the model-predicted distribution of Cr on the solid phase was found to be similar to that observed (Figure 1B). Since the model assumes a homogeneous porous media, the similarity is better than expected for a system known to be hydrologically and geochemically heterogeneous.

The mechanism of Cr retardation by the solid phase was identified using XANES spectroscopy (Figure 2a). XANES spectra were compiled for each extracted soil depth within the core, and they revealed that both Cr(VI) and Cr(III) resided on the solid phase. The preedge position at ~5994 eV is indicative of Cr(VI); the jump height, which represents the total atomic cross section, is indicative of the total Cr within the sample (*34*). Of the total influent Cr(VI) that was passed through the core, 24.4% was reduced to Cr(III). Of the total Cr residing on the solid phase, 58.8% was as Cr(III). Thus, these vadose zone soils, devoid of Fe(II)-bearing minerals, are capable of reducing Cr(VI) to Cr(III) in the presence of preferential flow and competing geochemical oxidation reactions. The latter is significant since these soils contain appreciable MnO_2 that can readily oxidize Cr(III) to Cr(VI), and they have shown sustained oxidation of $Co^{II}EDTA^{2-}$ to $Co^{III}EDTA^-$ (*22*). The lack of observable Cr(III) oxidation (no observable reduced Mn^{2+} products) is most likely the result of Cr(III) stabilization on amorphous Fe−oxides that dominate surface coatings in this soil and possibly due to a decreased oxidative potential of the Mn−oxides toward Cr(III) at pH < 5 (18). Further, X-ray absorption fine structure (XAFS) analysis of Cr dynamics in packed columns of these soils suggested that the immobilized Cr(III) exists on soil

TABLE 3. Parameter Estimates and Statistics Obtained during the Application of the Multireaction Transport Model (MRTM) to the Cr(VI) Displacement Experiments

column	K^b	n	k_{irr}, h^{-1}	r^2	irreversibly sorbed obsd, %	irreversibly sorbed pred,[c] %
Nonlinear Model[a]						
untreated	15.6± 2.0[d]	0.610 ± 0.047	0.0081 ± 0.0004	0.98	41.6	42.1
NOM amended	65.0 ± 15.4	0.391 ± 0.080	0.0083 ± 0.0008	0.90	54.2	55.9
Linear Model: $n = 1$						
untreated	5.38 ± 0.35[d]		0.0082 ± 0.0008	0.91		
NOM amended	9.91 ± 1.06		0.0093 ± 0.0011	0.81		

[a] Uses Freundlich isotherm. [b] K and n = empirical parameters from Freundlich equation; K = distribution coefficient when $n = 1$ (in $cm^3\ g^{-1}$); k_{irr} = irreversible first-order kinetic parameter. [c] From nonlinear model. [d] 95% confidence interval.

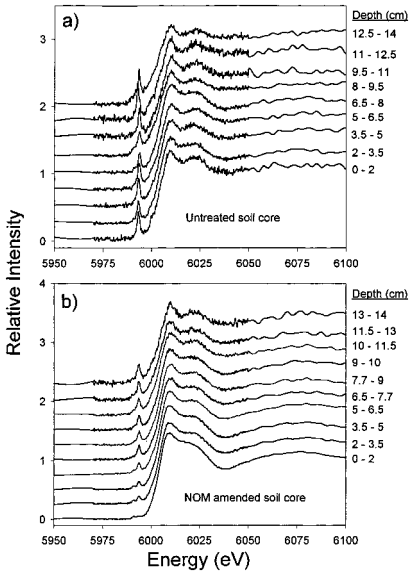

FIGURE 2. XANES spectra of (a) untreated and (b) NOM-amended soil cores as a function of depth following Cr(VI) displacement experiments. The intensity of the preedge white line (~5994 eV) relative to the total jump height is proportional to the fraction of Cr(VI) within the sample. Increasing fractions of Cr(VI) are noted by the increased preedge peak intensity at greater distances from the column inlet.

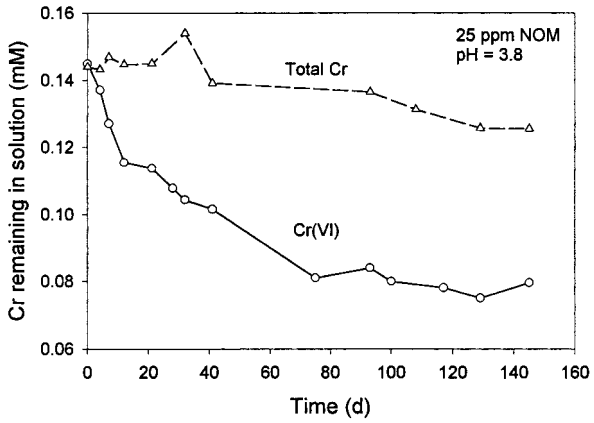

FIGURE 3. Loss of Cr(VI) as a function of time in a batch experiment containing an initial Cr(VI) concentration of 0.145 mM and 25 mg of C L^{-1} as natural organic matter at pH = 3.8.

mineral surfaces as strongly bound $Cr(OH)_3$ precipitates (Fendorf, Stanford University, unpublished data). The direct detection of the reduced product Cr(III) is consistent with the findings of James and Bartlett (*35*), who used indirect chemical methods to infer the formation of solid-phase Cr(III) from Cr(VI) reduction.

We speculate, therefore, that NOM residing on the solid phase causes the reduction of Cr(VI) to Cr(III). Sufficient surface-bound NOM exists in these systems (Table 1) to serve as a reductant for Cr(VI). Indirect NOM reduction mechanisms (Cr(VI) reduction by Fe(II) formed from NOM reduction of Fe(III)−oxides) as proposed by Anderson et al. (*10*) are unlikely due to the refractory (nonlabile) nature of the NOM in our system and the observation that no Fe was detected in the column effluent. Further, Deng and Stone (*7*) have verified the direct reduction of Cr(VI) by a variety of organics, with the redox reaction catalyzed by numerous types of oxide surfaces (e.g., TiO_2 > FeOOH ~ Al_2O_3). The acidic pH of the effluent (pH = 3.7) is not sufficiently low to promote the time-dependent aqueous-phase reduction of Cr(VI) to Cr(III), where H_2O serves as the reductant. At pH 3.7, the reduction kinetics of Cr(VI) to Cr(III) are extremely slow and solutions remain stable for time scales of months to years. Values of pH less than 3 are necessary to accelerate the reduction reaction in aqueous solution, and this can significantly confound the interpretation of experimental results such as those found in Eary and Rai (*8*, *9*).

Our speculation that NOM can effectively reduce Cr(VI) was supported by batch mixtures of dissolved NOM and Cr(VI) in the absence of solid-phase material (Figure 3). The NOM was obtained from a wetlands pond in Georgetown, SC (*28*), and has many of the same chemical features found in dissolved NOM derived from the A horizon of soils. It is primarily refractory in nature and consists of humic acid and fulvic acid macromolecules in the size range of 3−100*k* MW or greater. Chemical details of the NOM can be found in Gu et al. (*29*, *30*). Aqueous-phase Cr(VI) decreased exponentially with time in the presence of dissolved NOM, while the total Cr remained nearly constant (Figure 3). These results suggest Cr(VI) is being reduced to Cr(III), with NOM serving as the reductant. The rate of reduction is slow in this batch system with a time scale of days to months. The slow decline of total Cr with time suggests Cr(III) is potentially precipitating from solution after thousands of hours of reaction. The limited extent of this process results from the acidic aqueous pH and the possible inhibition of $Cr(OH)_3$ nucleation by NOM.

To test whether surface-bound NOM could effectively reduce Cr(VI), an additional undisturbed soil column with nearly identical features as those in Figure 1B was amended with dissolved NOM acquired from the wetland pond in Georgetown, SC (see Materials and Methods section). This treatment enhanced the original surface-bound NOM by nearly 2.2 times. The breakthrough of Cr on the NOM amended soil core was significantly more delayed than Cr breakthrough on the untreated soil (Figure 4A versus Figure 1A), suggesting greater Cr retention in the former. In fact, the time needed to reach an apparent plateau in the BTC ($C/C_0 \sim 0.6$) was nearly 1200 h longer for the NOM-amended

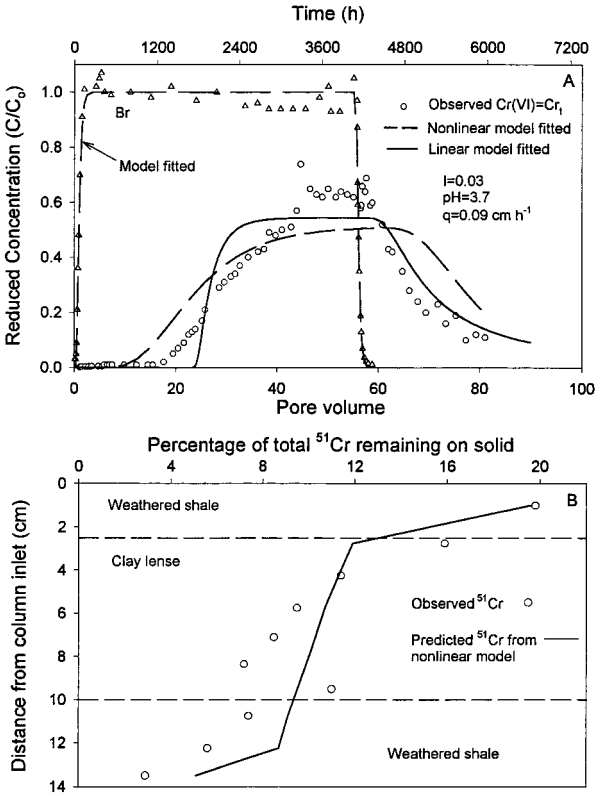

FIGURE 4. (A) Observed effluent Br^- and Cr(VI) with model-fitted curves using the multireaction transport model (MRTM) for an undisturbed soil column of interbedded weathered shale and clay lenses that was amended with natural organic matter (NOM). Model input and output parameters are provided in Tables 2 and 3. (B) Observed and predicted distribution of ^{51}Cr (Cr(III) and Cr(VI)) within the undisturbed column.

soil core. As with the untreated soil, effluent Cr was entirely Cr(VI) and ^{51}Cr behaved identical to stable Cr. The lack of effluent Cr(III) suggests that colloid-facilitated transport of Cr(III)−NOM complexes was of minor importance in these systems, most likely because these soils are efficient sorbents for NOM. Greater retardation of Cr species within the NOM-amended soil core was also evidenced by the fact that 54.2% of added Cr(VI) was irreversibly bound versus 41.6% in the untreated soil core (Table 3).

The effluent Cr(VI) BTC was modeled with MRTM in a similar manner as described for the untreated soil core. Model-fitted curves did not describe the observed data as well as for the untreated soil (Figure 4A versus Figure 1A and Table 3); however, the larger model-fitted K values for the NOM-amended soil relative to the untreated soil reflect the significantly increased retardation of the various Cr species due to added solid-phase NOM. Nevertheless, the overall modeling results were the same; nonlinear sorption more adequately described Cr(VI) breakthrough, and the addition of reversible first-order kinetic sites did not significantly improve the model fits. Based on the nonlinear model fit to Cr(VI) effluent, the model-predicted distribution of Cr on the solid phase was similar to that observed (Figure 4B) and showed similar trends to those of the untreated soil.

As with the untreated soil core, the mechanism of Cr retardation by the NOM-amended soil column was identified using XANES spectroscopy (Figure 2b). XANES spectra were compiled for each extracted soil depth within the core and showed that both Cr(VI) and Cr(III) resided on the solid phase. The XANES results further revealed that significantly less Cr(VI) was present in the NOM-amended soil core versus the untreated soil core (Figure 2b vs Figure 2a). For the NOM-

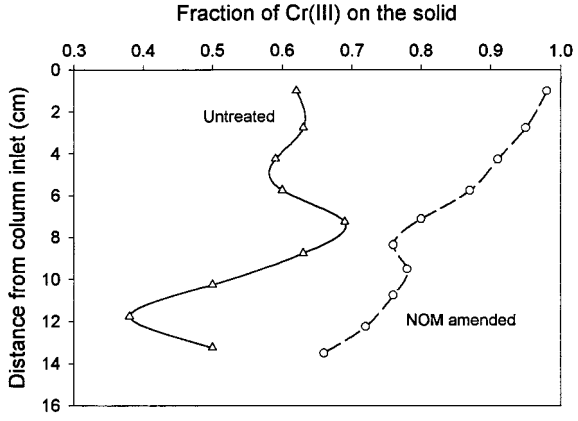

FIGURE 5. Fraction of the reduced Cr(III) product that was formed as a function of depth in the untreated and natural organic matter (NOM) amended soil columns during the Cr(VI) displacement experiments.

amended soil, 84.5% of the solid-phase Cr was as Cr(III). This was significantly greater than the 58.8% observed in the untreated soil. In fact, of the total Cr(VI) that passed through the columns, 45.8% was reduced to Cr(III) in the NOM-amended soil compared to 24.4% in the untreated soil. The increased magnitude of Cr(VI) reduction on the NOM-amended soil compares favorably with the extent of additional NOM added (a 2.2-fold increase).

The influence of surface-bound NOM on the reduction of Cr(VI) to Cr(III) is shown clearly in Figure 5. The fraction of Cr(III) on the solid phase is consistently greater on the NOM-amended soil versus the untreated soil for any given depth within the core. The reduction of Cr(VI) to Cr(III) in both soils is greater near the column inlet and decreases with increasing depth; however, the extent of reduction is much more dramatic in the NOM-amended soil. In fact, within the first 8 cm of the NOM-amended core, Cr(VI) reduction ranges from >96% near the column inlet to 80% midway through the column. The decreased reduction of Cr(VI) with depth in the soil cores is consistent with decreasing solid-phase NOM with depth, which was measured after the tracer displacement experiments (not shown). These values most likely represent the initial NOM in the system as well, since significant carbon pulses were never detected in the effluent. Since complete oxidation of NOM to $CO_{2(g)}$ is doubtful, these observations suggest that solid-phase carbon was conserved during the redox reaction.

The rate of Cr(VI) reduction by NOM was significantly more rapid in the presence of the soil solid phase versus batch reactions devoid of mineral surfaces. Batch Cr(VI) reduction by NOM (Figure 3) was modeled as a first-order irreversible reaction, and a model-fitted k_{irr} value of $2.5 \times 10^{-4} \pm 5 \times 10^{-5}$ h^{-1} ($r^2 = 0.90$) was obtained. This value was nearly 35 times smaller than model k_{irr} values established for Cr(VI) reduction for the two soil cores (Table 3). The results suggest that the soil mineral surfaces may serve to catalyze the reduction of Cr(VI) to Cr(III), which is in agreement with the findings of Deng and Stone (*6*, *7*), who have shown common mineral oxides catalyze Cr(VI) reduction by organics.

Environmental Significance

This study has shown that surface-bound NOM (e.g., humics and fulvics) can effectively reduce Cr(VI) to Cr(III) in undisturbed highly acidic field soils (i.e., pH ~ 4) even in the presence of competing hydrologic and geochemical processes. The reduction reaction is catalyzed by the presence of soil mineral surfaces, and the reduced product Cr(III) is immobilized as tightly bound surface species (adsorption

and $Cr(OH)_3$ precipitation products). The rate of immobilization is rapid with half-lives on the order of 85 h. At typical pore water fluxes within the vadose zone, the rapid immobilization rate will limit the downward vertical migration in soils. In acidic soils where the pH is ≤4, the availability of even small amounts of surface-bound NOM (0.05% w/w on the solid) along soil flow paths can dramatically impede the mobility of Cr(VI) in the environment. Organic amendments to Cr(VI)-contaminated acidic soils could easily be engineered into an effective remedial strategy targeted at Cr immobilization.

Acknowledgments

This research was sponsored by the U.S. Department of Energy, Office of Biological and Environmental Research, Environmental Technology Partnership Program. We appreciate the efforts of Dr. Paul Bayer, the contract officer for the Department of Energy who supported this work. XANES analysis was conducted at the Stanford Synchrotron Radiation Laboratory (SSRL), which is operated by the Department of Energy, Office of Basic Energy Sciences. The SSRL Biotechnology Program is supported by the National Institutes of Health, National Center for Research Resources, Biomedical Technology Program, and by the Department of Energy, Office of Biological and Environmental Research. Oak Ridge National Laboratory is managed by Lockheed Martin Energy Research Corp. under Contract DE-AC05-96OR22464 with the U.S. Department of Energy. This is Environmental Science Division, ORNL, publication no. 4914.

Literature Cited

(1) Amacher, M. C.; Kotuby-Amacher, J.; Selim, H. M.; Iskandar, I. K. *Geoderma* **1986**, *38*, 131−154.
(2) Losi, M. E.; Amrhein, C.; Frankenberger, W. T., Jr. *J. Environ. Qual.* **1994**, *23*, 1141−1150.
(3) Powell, R. M.; Puls, R. W.; Hightower, S. K.; Sabatini, D. A. *Environ. Sci. Technol.* **1995**, *29*, 1913−1922.
(4) Davis, A.; Olsen, R. L. *Groundwater* **1995**, *33*, 759−768.
(5) Fendorf, S. E.; Li, G. *Environ. Sci. Technol.* **1996**, *30*, 1614−1617.
(6) Deng, B.; Stone, A. T. *Environ. Sci. Technol.* **1996**, *30*, 463−472.
(7) Deng, B.; Stone, A. T. *Environ. Sci. Technol.* **1996**, *30*, 2484−2494.
(8) Eary, L. E.; Rai, D. *Am. J. Sci.* **1989**, *289*, 180−213.
(9) Eary, L. E.; Rai, D. *Soil Sci. Soc. Am. J.* **1991**, *55*, 676−683.
(10) Anderson, L. D.; Kent, D. B.; Davis, J. A. *Environ. Sci. Technol.* **1994**, *28*, 178−185.
(11) Peterson, M. L.; Brown, G. E., Jr.; Parks, G. A.; Stein, C. L. *Geochim. Cosmochim. Acta* **1997**, *61*, 3399−3412.
(12) Barlett, R. J.; Kimble, J. M. *J. Environ. Qual.* **1976**, *5*, 383−386.
(13) Stewart, R. *Oxidation Mechanisms: Application to Organic Chemistry;* W. A. Benjamin, Inc.: New York, 1964.
(14) Cainelli, G.; Cardillo, G. *Chromium Oxidations in Organic Chemistry;* Springer-Verlag: New York, 1984.
(15) Kent, D. B.; Davis, J. A.; Anderson, L. C. D.; Rea, B. A. *Water Resourc. Res.* **1994**, *30*, 1099−1114.
(16) Kent, D. B.; Davis, J. A.; Anderson, L. C. D.; Rea, B. A. *Water Resourc. Res.* **1995**, *31*, 1041−1050.
(17) Selim, H. M.; Amacher, M. C.; Iskandar, I. K. *Modeling the Transport of Heavy Metals in Soils;* Monograph 90−2; U.S. Army Corps of Engineers: Hanover, NH, 1990.
(18) Fendorf, S. E.; Zasoski, R. J. *Environ. Sci. Technol.* **1992**, *26*, 79−85.
(19) Arnseth, R. W.; Turner, R. S. *Soil Sci. Soc. Am. J.* **1988**, *52*, 1801−1807.
(20) Jardine, P. M.; Wilson, G. V.; Luxmoore, R. J. *Soil Sci. Soc. Am. J.* **1988**, *52*, 1252−1259.
(21) Jardine, P. M.; Jacobs, G. K.; Wilson, G.V. *Soil Sci. Soc. Am. J.* **1993a**, *57*, 945−953.
(22) Jardine, P. M.; Jacobs, G. K.; O'Dell, J. D. *Soil Sci. Soc. Am. J.* **1993b**, *57*, 954−962.
(23) Wilson, G. V.; Luxmoore, R. J. *Soil Sci. Soc. Am. J.* **1988**, *52*, 329−335.
(24) Wilson, G. V.; Alfonsi, J. M.; Jardine, P. M. *Soil Sci. Soc. Am. J.* **1989**, *53*, 679−685.
(25) Wilson, G. V.; Jardine, P. M.; Gwo, J. P. *Soil Sci. Soc. Am. J.* **1992**, *56*, 1731−1737.
(26) Wilson, G. V.; Jardine, P. M.; O'Dell, J. D.; Collineau, M. *J. Hydrol.* **1993**, *145*, 83−109.
(27) Reedy, O. C.; Jardine, P. M.; Wilson, G. V.; Selim, H. M. *Soil Sci. Soc. Am. J.* **1996**, *60*, 1376−1384.
(28) McCarthy, J. F.; Williams, T. M.; Liang, L.; Jardine, P. M.; Jolley, L. W.; Taylor, D. L.; Palumbo, A. V.; Cooper, L. W. *Environ. Sci. Technol.* **1993**, *27*, 667−676.
(29) Gu, B.; Schmitt, J.; Chen, Z.; Liang, L.; McCarthy, J. F. *Environ. Sci. Technol.* **1994**, *28*, 38−46.
(30) Gu, B.; Schmitt, J.; Chen, Z.; Liang, L.; McCarthy, J. F. *Geochim. Cosmochim. Acta* **1995**, *59*, 219−229.
(31) Jardine, P. M.; Weber, N. L.; McCarthy, J. F. *Soil Sci. Soc. Am. J.* **1989**, *53*, 1378−1385.
(32) Larsen, I. L.; Cutshall, N. H. *Earth Planet. Sci. Lett.* **1981**, *54*, 379−384.
(33) Cramer, S. P.; Tench, O.; Yocum, M.; George, G. N. *Nucl. Instr. Methods Phys.* **1988**, *A266*, 586−591.
(34) Patterson, R. R.; Fendorf, S.; Fendorf, M. *Environ. Sci. Technol.* **1997**, *31*, 2039−2044.
(35) James, B. R.; Bartlett, R. J. *J. Environ. Qual.* **1983**, *12*, 177−181.
(36) Mehra, O. P.; Jackson, M. L. *Clays Clay Miner.* **1960**, *7*, 317−327.

Received for review November 23, 1998. Revised manuscript received June 15, 1999. Accepted June 21, 1999.

ES981211V